Acta Crystallographica Section A
Foundations of Crystallography
ISSN 0108-7673

Received 31 March 2008
Accepted 6 May 2008

Estimated H-atom anisotropic displacement parameters: a comparison between different methods and with neutron diffraction results

Parthapratim Munshi,[a] Anders Ø. Madsen,[b,c] Mark A. Spackman,[a]* Sine Larsen[b,c] and Riccardo Destro[d]

[a]University of Western Australia, Australia, [b]University of Copenhagen, Denmark, [c]European Synchrotron Radiation Facility, France, and [d]University of Milan, Italy. Correspondence e-mail: mark.spackman@uwa.edu.au

Anisotropic displacement parameters (ADPs) are compared for H atoms estimated using three recently described procedures, both among themselves and with neutron diffraction results. The results convincingly demonstrate that all methods are capable of giving excellent results for several benchmark systems and identify systematic discrepancies for several atom types. A revised and extended library of internal H-atom mean-square displacements is presented for use with Madsen's SHADE web server [*J. Appl. Cryst.* (2006), **39**, 757–758; http://shade.ki.ku.dk], and the improvement over the original SHADE results is substantial, suggesting that this is now the most readily and widely applicable of the three approximate procedures. Using this new library – SHADE2 – it is shown that, in line with expectations, a segmented rigid-body description of the heavy atoms yields only a small improvement in the agreement with neutron results. The SHADE2 library, now incorporated in the SHADE web server, is recommended as a routine procedure for deriving estimates of H-atom ADPs suitable for use in charge-density studies on molecular crystals, and its widespread use should reveal remaining deficiencies and perhaps overcome the inherent bias in the majority of such studies.

1. Introduction

Charge-density analysis of accurate X-ray diffraction data is being used increasingly to extract *quantitative* information on chemical bonding and the properties of molecules in crystals, and those experiments are unique in their potential to provide such detailed three-dimensional information on the solid state. Obtaining accurate and reliable electron distributions currently relies heavily on the atom-centred multipole formalism and a satisfactory deconvolution of the modelled electron density from the motion of the nuclei about which it is expanded. In this context, it is worthy of note that quantities derived from a topological analysis of the modelled electron distribution, based on Bader's quantum theory of atoms in molecules (QTAM) (Bader, 1990), are now the focus of more than 90% of current charge-density publications. Although such analyses are relatively easy to perform with modern software, it should not be forgotten that, because it depends intimately on the second derivative of the electron density, QTAM demands extremely high quality in the modelled electron density; artefacts will necessarily result in spurious and even erroneous results. And artefacts can arise from systematic errors in the diffraction data, deficiencies in the multipole model itself, or from an inadequate description of the nuclear motion. We are concerned in this work with the treatment of nuclear motion, which typically relies on the harmonic approximation and, most generally, in the form of anisotropic displacement parameters (ADPs). In their recent review summarizing a variety of chemical applications of charge-density analysis, Koritsanszky & Coppens (2001) devoted only a few brief paragraphs to the importance of obtaining an accurate description of nuclear motion. However, their comments are worth repeating: 'Owing to their low scattering power and intense thermal motion, H atoms should be treated with special care. The use of independent observations, mainly neutron diffraction parameters, is a clear advantage, providing systematic differences between neutron and X-ray thermal parameters are properly taken into account. The physical significance of the ADPs of non-hydrogen atoms is also an important issue. An inadequate density model manifests itself in unreliable estimates for the ADPs or, in other words, *no reasonable estimate of the charge-density parameters can be obtained without an adequate description of thermal motion.*' (emphasis in the original text).

Given the importance of a reliable description of thermal motion, especially for H atoms, and the evident appreciation of this within the charge-density community, it is surprising that a review of the literature for the years 1999–2007 reveals

that 82% of charge-density studies on molecules containing hydrogen treated H atoms with an isotropic thermal motion model. Complementary neutron diffraction results were used to provide H-atom ADPs for 13% of studies, while 5% (11 studies) estimated H-atom ADPs from a combination of rigid-body analysis of the heavy-atom skeleton, augmented with estimates of 'internal' mean-square displacements of H atoms along and perpendicular to X—H bonds. Fig. 1 summarizes the statistics for the 9 year period, and from it we conclude that there is no evidence of a trend away from the *status quo*, *i.e.* relying almost solely on an isotropic description of H-atom thermal motion. In fact, it could be argued that there is a recent trend *away* from an anisotropic description of the motion of H atoms. Through this publication, we aim to improve this situation by demonstrating that present methods are not only available for the routine estimation of H-atom ADPs in a wide range of molecular crystals but their results compare well with one another and with neutron diffraction results. In performing this comparison, we also identify strengths and weaknesses of the present methods, and as a result implement some improvements as well as indicate directions in which further improvements may be made in the future.

2. A brief description of estimation methods

It would appear that all methods so far employed to estimate ADPs for H atoms spring from a suggestion originally due to Hirshfeld (1976). At its simplest, a rigid-body model is used to describe the motion of the heavy-atom skeleton of the molecule, and the H atoms are then assumed to follow the motion of this rigid frame. For computational purposes, the H nuclei are usually placed at average neutron bond lengths. Thus, the rigid-body analysis of X-ray heavy-atom ADPs is used to estimate 'external' contributions to the ADPs of H atoms, and to this the 'internal' contributions are added for each H atom, $U^{ij} = U^{ij}_{\rm internal} + U^{ij}_{\rm external}$. By far the most common method for estimating the external contributions to the ADPs is the rigid-body or TLS analysis (Schomaker & Trueblood, 1968), although some more complex molecules have been analysed using the segmented rigid-body approach with attached rigid groups (Schomaker & Trueblood, 1998). Implementations of Hirshfeld's idea differ mostly in the way in which the internal mean-square displacements of the H atoms are approximated.

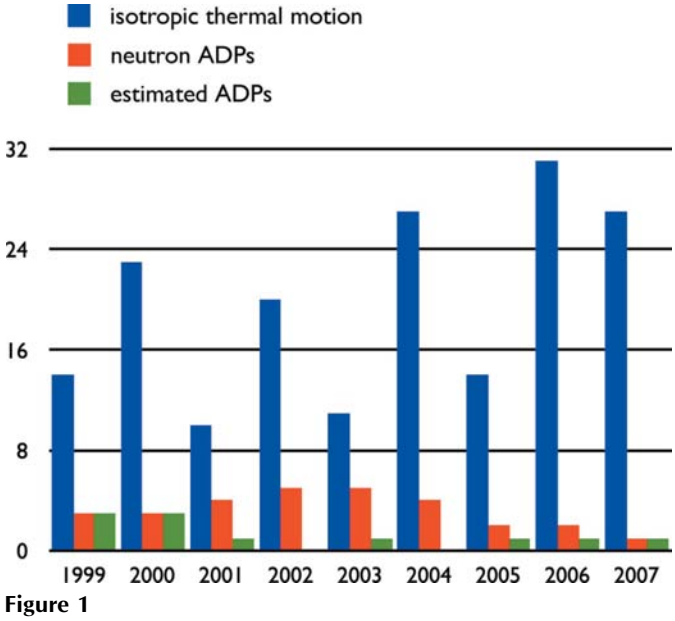

Figure 1
Histogram summarizing treatment of H-atom thermal motion in charge-density studies published for the period 1999–2007.

The earliest reports using estimated H-atom ADPs appear in charge-density studies from Hirshfeld's group. For diformohydrazide and formamide (Eisenstein, 1979) and 2-cyanoguanidine (Hirshfeld & Hope, 1980), internal estimates were obtained from spectroscopic frequencies and normal modes for isolated formamide and *N*-methylacetamide molecules, while for the bicyclobutane derivative (Eisenstein & Hirshfeld, 1983) a segmented TLS model was used along with internal estimates from spectroscopic data on methanol. In a later study on cytosine and adenine (Eisenstein, 1988), internal mean-square displacements (MSDs) came from neutron diffraction data for 9-methyladenine (McMullan *et al.*, 1980) and gas-phase spectroscopic data for cytosine. Baert and co-workers have also employed Hirshfeld's approach, with estimates of internal MSDs obtained from infrared and Raman spectroscopy, in their charge-density analyses of a series of NLO materials [3-methyl-4-nitropyridine-*N*-oxide (POM) (Baert *et al.*, 1988), *N*-(4-nitrophenyl)-L-prolinol (NPP) (Fkyerat *et al.*, 1995), *m*-nitrophenol (Hamzaoui *et al.*, 1996) and 2-amino-5-nitropyridinium dihydrogen phosphate (2A5NPDP) (Puig-Molina *et al.*, 1998)]. Although Craven's group typically undertook neutron diffraction experiments to complement their X-ray diffraction data, where this was not possible they also estimated H-atom ADPs. Thus, for ammonium dimethylphosphate (Klooster & Craven, 1992), internal estimates for methyl and ammonium H atoms were obtained from neutron data on related crystal structures, and for β-cytidine (Chen & Craven, 1995) a segmented TLS model was combined with internal estimates from a neutron study on adenosine (Klooster *et al.*, 1991).

Although it is not obvious at first sight, an equivalent approach was used in a number of charge-density analyses reported by Koritsanszky and co-workers. It involved the determination of starting ADPs for all atoms in a molecule from normal modes and vibrational frequencies obtained from an *ab initio* geometry optimization for an isolated molecule. In the subsequent multipole refinement against X-ray data, shifts in the ADPs were constrained using a large number ($6N - 20$, where N is the number of atoms in the molecule) of rigid-link constraints. Studies on D,L-aspartic acid (Flaig *et al.*, 1998), a semibullvalene (Williams *et al.*, 1999), diisocyanomethane (Koritsanszky *et al.*, 1999), 1,1-difluoroallene (Buschmann *et al.*, 2000) and potassium hydrogen tartrate (Koritsanszky *et al.*, 2000) all employed this strategy, and in some of them the authors note that complications can arise from a different conformation in the crystal compared with that obtained for an isolated molecule.

In the present work, we choose to compare results from three methods that have been recently described for the estimation of H-atom ADPs: the empirical approaches of Roversi & Destro (2004) and Madsen *et al.* (2004), and the theoretical approach of Whitten & Spackman (2006). Details of the methods, and especially the assumptions and earlier work upon which they are based, are provided in those works and in others cited below.

2.1. ADPH

Half of the studies for the period 1999–2007 reporting estimated H-atom ADPs were from Destro's group in Milan. In those analyses, estimates of internal contributions to the MSDs of H atoms were deduced from mean-square amplitudes of motion for approximate vibrational modes and frequencies obtained from solid-state infrared spectra. The molecules investigated in this manner were α-glycine (Destro *et al.*, 2000), 3,4-bis(dimethylamino)-3-cyclobutene-1,2-dione (DMACB) (May *et al.*, 2001), a push–pull ethylene (PPE; although here the 'spectroscopic' data came from HF/6-31G* optimized geometry of PPE, and experimental frequencies for the water molecule) (Forni & Destro, 2003), an angiotensin receptor antagonist (Destro *et al.*, 2005; Soave *et al.*, 2007), and a fungal metabolite (Lo Presti *et al.*, 2006). Earlier studies also include *syn*-1,6:8,13-biscarbonyl[14]annulene (BCA; although internal motion here was chosen to be 0.0065, 0.0145 and 0.0240 Å^2 for C—H stretch, in-plane and out-of-plane bending, obtained from Hirshfeld and based on a normal-coordinate calculation for anthracene) (Destro & Merati, 1995) and citrinin (Roversi *et al.*, 1996). This approach has been recently implemented in the code ADPH and described in detail by Roversi & Destro (2004). Although it is in principle quite widely applicable, it relies on the availability of relevant solid-state spectroscopic data or, in their absence, the transferability of frequencies and normal modes from isolated molecules containing similar functional groups to the specific molecule of interest in the solid state.

2.2. SHADE

A standardized approach using neutron diffraction estimates of internal MSDs for H atoms – along the lines of earlier work from Craven's group – was described by Madsen *et al.* (2004), and tested in some detail on charge-density analyses on methylammonium hydrogensuccinate monohydrate (MAHS), methylammonium hydrogenmaleate (MADMA), urea and xylitol. Separate analyses of high-quality neutron diffraction studies, mainly on carbohydrates, were used to establish a database of internal MSDs for H atoms (Madsen *et al.*, 2003). The database in its original form included results for methyl, methylene, methine, hydroxy, water and ammonium H atoms. Aromatic H atoms were assigned the same values as methine H atoms and, for atoms not in any of the above bonding environments, default values of 0.005 Å^2 (bond direction) and 0.020 Å^2 (perpendicular to the bond) were assigned. This procedure has been made available as a convenient web server, where it has been given the acronym SHADE (simple hydrogen anisotropic displacement estimator) (Madsen, 2006; http://shade.ki.ku.dk). The SHADE approach is perhaps the most readily applicable to larger molecules but it relies on the accuracy of assuming three normal modes (along and perpendicular to the X—H bond) and it depends greatly on the assumption of transferability of internal MSDs from one crystal to another, something that has been demonstrated to be only approximately valid.

2.3. TLS + ONIOM

In an attempt to overcome the difficulties that arise when *ab initio* calculations result in an optimized molecular geometry that is very different from that observed in the crystal [*e.g.* xylitol (Madsen *et al.*, 2003) and the hexanoate anion (Luo *et al.*, 1996)], Whitten & Spackman (2006) have recently described the use of the ONIOM cluster method (Svensson *et al.*, 1996; Dapprich *et al.*, 1999; Vreven *et al.*, 2003, 2006) to mimic the local environment experienced by a molecule in a crystal. That approach employs a Hartree–Fock description of the molecule of interest, surrounded by a layer of nearest-neighbour molecules. The outer layer of molecules is described by a simple molecular-mechanics force field, with point charges on the atoms chosen to best fit the electric field from a periodic Hartree–Fock calculation on the crystal (Whitten *et al.*, 2006). In this manner, the internal motion of the atoms is described at the Hartree–Fock level, while the interaction between the central molecule and its neighbours – including the important hydrogen bonds – is described at the molecular mechanics level. The method was denoted TLS + ONIOM and ADPs computed in this manner agreed favourably with neutron results for 1-methyluracil, α-glycine, xylitol and 2-methyl-4-nitroaniline (MNA). In principle, the TLS + ONIOM approach is capable of the most accurate results but as originally described it requires a periodic Hartree–Fock calculation on the crystal, as well as an ONIOM geometry optimization of a cluster, typically of ~15 molecules. Potential-derived charges obtained for an isolated molecule have also been used instead of field-derived charges for sarcosine (Dittrich & Spackman, 2007) and adenosine (Osborne, 2006).

The TLS + ONIOM method also differs from the other two in a more subtle way. Before the TLS model is fitted against the X-ray derived ADPs for the heavy atoms, internal contributions deduced from the $3N - 6$ highest frequencies and normal modes of the ONIOM cluster calculation are subtracted from the X-ray results. As noted by Whitten & Spackman (2006), this apparently small correction always reduces the root-mean-square value of MSD amplitudes along interatomic directions for all pairs of atoms.

3. Detailed comparison with neutron diffraction results

We compare in some detail the results from the three chosen methods with adjusted neutron data, and with one another, for five molecular crystals; relevant experimental details are summarized in the first five entries of Table 1. With the exception of L-alanine, these crystals were part of the original

Table 1
Summary of molecular crystals and experimental diffraction data chosen for the comparisons.

Crystal	Formula	Space group	X-ray data		Neutron data	
			T (K)	Ref.	T (K)	Ref.
α-Glycine	$C_2H_5NO_2$	$P2_1/n$	23	(*a*)	15	(*b*)
1-Methyluracil	$C_5H_6N_2O_2$	*Ibam*	21	(*c*)	15	(*d*)
L-Alanine	$C_3H_7NO_2$	$P2_12_12_1$	23	(*e*)	60	(*f*)
2-Methyl-4-nitroaniline	$C_7H_8N_2O_2$	*Ia*	10	(*g*)	100	(*g*)
Xylitol	$C_5H_{12}O_5$	$P2_12_12_1$	122	(*h*)	122	(*i*)
MBADNP	$C_{13}H_{12}N_4O_4$	$P2_1$	20	(*j*)	20	(*j*)
Adenosine	$C_{10}H_{13}N_5O_4$	$P2_1$	100	(*k*)	123	(*l*)
Nit(SMe)Ph	$C_{14}H_{19}N_2O_2S$	$P2_1/a$	114	(*m*)	114	(*m*)
Austdiol	$C_{12}H_{12}O_5$	$P2_12_12$	70	(*n*)		
Push–pull ethylene (PPE)	$C_{14}H_{24}N_2O_2{\cdot}H_2O$	$Pna2_1$	21	(*o*)		
Milfasartan	$C_{30}H_{30}N_6O_3S$	*Pbca*	17	(*p*)		

References: (*a*) Destro *et al.* (2000); (*b*) Kvick (1993); (*c*) Roversi & Destro (2004); (*d*) McMullan & Craven (1989); (*e*) Destro *et al.* (1988); (*f*) Wilson *et al.* (2005); (*g*) Whitten *et al.* (2006); (*h*) Madsen *et al.* (2004); (*i*) Madsen *et al.* (2003); (*j*) Cole *et al.* (2002); (*k*) Hübschle (2007); (*l*) Klooster *et al.* (1991); (*m*) Pillet *et al.* (2001); (*n*) Lo Presti *et al.* (2006); (*o*) Forni & Destro (2003); (*p*) Destro *et al.* (2005).

TLS + ONIOM paper, where the focus was on comparison with neutron diffraction results. Since that work was published, we have become aware of neutron results for α-glycine at 15 K (Kvick, 1993) and at 20 K (Klooster *et al.*, 1996), as well as L-alanine at 60 K (Wilson *et al.*, 2005), and those results form part of an important benchmark for the present comparison. For the present study, we have performed a TLS + ONIOM calculation on L-alanine using the original procedure and for all five systems we have used the original SHADE web server to compute results for comparison. For three systems – α-glycine, L-alanine and 1-methyluracil – we also compare with results obtained with ADPH. As neutron diffraction results serve as our benchmark in this comparison, it is important to note that we adjust the neutron ADPs for all atoms in such a way that those for heavy atoms are in better agreement with those obtained from the X-ray diffraction data, $\mathbf{U}_{\rm neutron} = q\mathbf{U}_{\rm X\text{-}ray} + \Delta\mathbf{U}$, using Blessing's approach as coded in *UIJXN* (Blessing, 1995).[1] This adjustment is usually relatively small but it can highlight systematic differences between the X-ray and neutron results. For example, in the present case, the scale factor q is within 5% of unity for 1-methyluracil, MNA and xylitol, while for L-alanine it is 0.831, reflecting the temperature difference of 37 K between the X-ray and neutron experiments (Table 1).

Figs. 2–6 present *ORTEP* representations of the adjusted neutron ADPs alongside TLS + ONIOM, SHADE and ADPH results (where available). For each H atom, the figures also include a value of the *similarity index* S_{12}, in each case a measure of the agreement of the estimated ADP for that atom with the adjusted neutron result. This index was introduced by Whitten & Spackman (2006) and is given by the expression

[1] Supplementary data, including values of q and ΔU, adjusted neutron, SHADE, SHADE2, TLS + ONIOM and ADPH ADPs for each molecular crystal are available from the IUCr electronic archives (Reference: SH5076). Services for accessing these data are described at the back of the journal.

Table 2
Mean values of similarity indices, $\bar{S}$, and $\Delta U^{\rm iso}$ ($\times 10^4$ Å^2, the mean difference in $U^{\rm iso}$ for the two sets of H-atom ADPs) for comparing estimated H-atom ADPs with benchmark neutron diffraction results.

Crystal	TLS + ONIOM		ADPH		SHADE		SHADE2	
	$\bar{S}$	$\Delta U^{\rm iso}$	$\bar{S}$	$\Delta U^{\rm iso}$	$\bar{S}$	$\Delta U^{\rm iso}$	$\bar{S}$	$\Delta U^{\rm iso}$
α-Glycine	0.71	5	0.68	−16	0.80	3	0.62	7
1-Methyluracil	0.16	−6	0.34	6	0.85	9	0.44	12
L-Alanine	0.84	35	0.75	8	1.79	49	1.30	45
2-Methyl-4-nitroaniline	0.45	11			0.68	12	0.40	11
Xylitol	0.65	−4			0.56	−13	0.56	−10

$S_{12} = 100(1 - R_{12})$, where R_{12} is a measure of the overlap between the probability density functions (p.d.f.'s) described by two ADPs, $\mathbf{U}_1$ and $\mathbf{U}_2$:

$$R_{12} = \int \sqrt{p_1(\mathbf{x})p_2(\mathbf{x})}\,{\rm d}^3\mathbf{x} = \frac{2^{3/2}(\det \mathbf{U}_1^{-1}\mathbf{U}_2^{-1})^{1/4}}{[\det(\mathbf{U}_1^{-1} + \mathbf{U}_2^{-1})]^{1/2}}. \quad (1)$$

Because the p.d.f.'s are normalized, $R_{12} = 1.0$ if $\mathbf{U}_1$ and $\mathbf{U}_2$ are identical, and hence S_{12} is a convenient (and coordinate-system-independent) measure of the percentage difference between the two p.d.f.'s; the smaller the value of S_{12}, the more similar the two p.d.f.'s are, and the closer the agreement between the ADPs $\mathbf{U}_1$ and $\mathbf{U}_2$. The figures also provide values of the mean similarity index, $\bar{S}$, for each approximate method compared with the adjusted neutron results. Mean similarity indices for comparisons against neutron results, and between the different estimation methods, are given in Table 2, while Table 3 provides a breakdown of mean similarity indices (against neutron results) as a function of atom type. Although the similarity index provides an immediate measure of the level of agreement of one ADP tensor with another, it doesn't provide information on *how* the two ADPs differ. One of the most important systematic differences can be discerned by comparing equivalent isotropic U values derived from the ADPs, $U^{\rm iso} = \frac{1}{3}(U_1 + U_2 + U_3)$ (where U_1, U_2 and U_3 are the principal components of the ADP tensor), and hence deviations from the reference neutron values $\Delta U^{\rm iso} =$

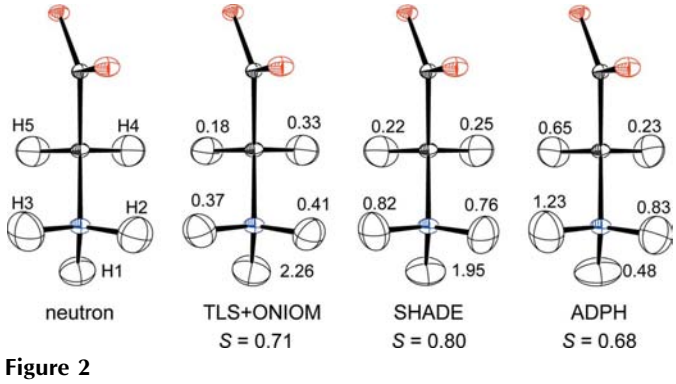

Figure 2
ORTEP comparison of estimated H-atom ADPs (23 K) with neutron results for α-glycine. Ellipsoids are 75% probability surfaces and are coloured for N (blue) and O (red) atoms, while those for H atoms are shown only with principal directions.

Table 3
Breakdown by atom type for mean similarity indices compared with neutron, $\bar{S}$, and deviations of U^{iso} ($\times 10^4$ Å^2) from neutron results for estimated H-atom ADPs.

	TLS + ONIOM			ADPH			SHADE			SHADE2		
Atom type	$\bar{S}$	ΔU^{iso}	N	$\bar{S}$	ΔU^{iso}	N	$\bar{S}$	ΔU^{iso}	N	$\bar{S}$	ΔU^{iso}	N
–C–H aliphatic	0.30	−1	4	0.46	4	1	0.28	6	4	0.31	8	4
–C–H aromatic	0.30	11	5	0.19	13	2	0.50	−11	5	0.46	17	5
–CH–H	0.70	−29	6	0.44	−13	2	0.68	−10	6	0.71	–8	6
–CH_2–H	0.43	8	8	0.51	−11	5	1.51	50	8	0.85	34	8
–N–H	0.06	7	1	0.30	25	1	1.69	53	1	0.80	39	1
–NH–H	1.00	31	2				0.79	9	2	0.48	–13	2
–NH_2–H	1.00	25	6	0.90	2	6	1.23	5	6	0.95	10	6
–O–H	0.67	24	5				0.51	−12	5	0.45	–9	5
Mean for all 37 atoms	0.59	7					0.89	9		0.66	10	
Mean for 17 atoms in common	0.60	14		0.59	−1		1.22	24		0.85	24	

U^{iso}(estimated) − U^{iso}(neutron) (see supplementary material). Table 3 also provides a breakdown of these average values by atom type for each of the three methods.

We briefly discuss the most important points that emerge from an examination of Figs. 2–6 and Tables 2 and 3, and follow this with an overview of the results.

***α*-Glycine**. The (unpublished) neutron H-atom ADPs for α-glycine present a dilemma. Those from Kvick (1993) were not accompanied by heavy-atom ADPs, making it impossible to make any adjustment using *UIJXN*. On the other hand, a comparison between heavy-atom ADPs from Klooster *et al.* (1996) and X-ray results from Destro *et al.* (2000) results in a scale factor q = 0.785, despite the two experiments being performed at close to 20 K. Combined with the fact that there are large differences between scale factors obtained for individual U^{ii} components (from 0.700 for U^{11} to 0.937 for U^{33}), this suggests that any scaling on this basis is likely to be extremely unreliable. We therefore decided to use the comparison with estimated results to assess the best neutron benchmark H-atom ADPs from a choice between: (i) unadjusted from Kvick (1993); (ii) unadjusted from Klooster *et al.* (1996); and (iii) adjusted from Klooster *et al.* (1996). The resulting $\bar{S}$ values (averaged over TLS + ONIOM, SHADE and ADPH) are 0.73 for (i), 1.06 for (ii) and 1.47 for (iii), clearly showing that the unadjusted values from Kvick (1993) are the most appropriate for our purposes. Fig. 2 shows that

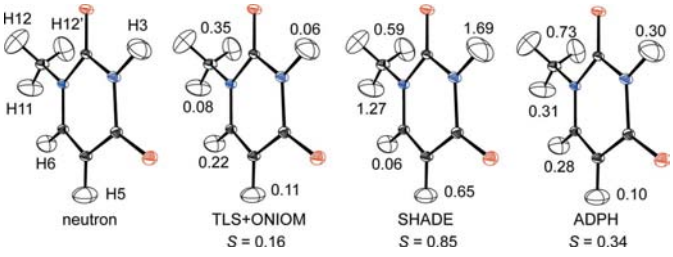

Figure 3
ORTEP comparison of estimated H-atom ADPs (21 K) with adjusted neutron results for 1-methyluracil. Ellipsoids as in Fig. 2.

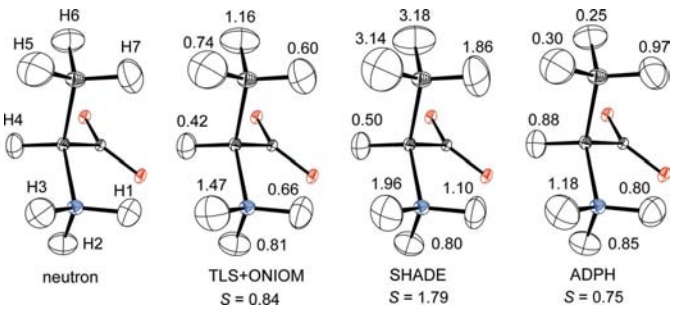

Figure 4
ORTEP comparison of estimated H-atom ADPs (23 K) with adjusted neutron results for L-alanine. Ellipsoids as in Fig. 2.

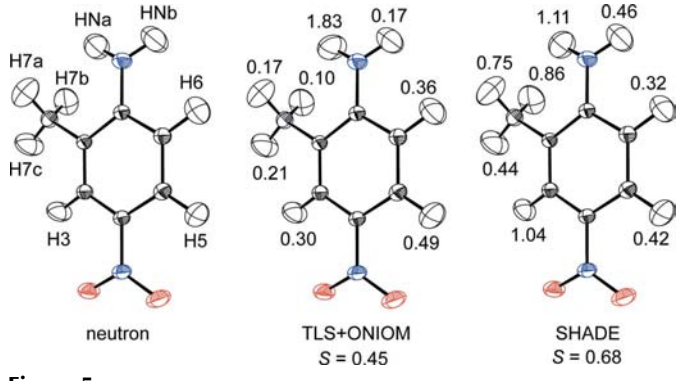

Figure 5
ORTEP comparison of estimated H-atom ADPs (100 K) with adjusted neutron results for 2-methyl-4-nitroaniline. Ellipsoids as in Fig. 2.

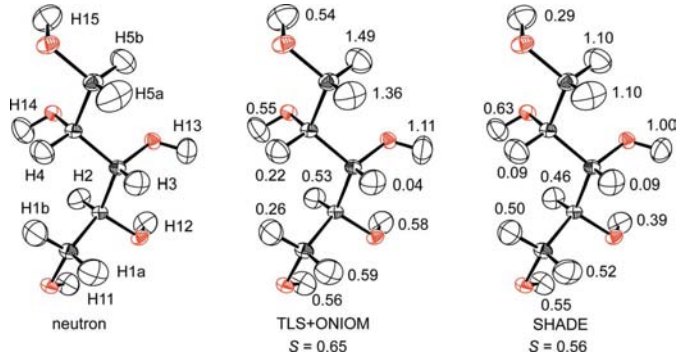

Figure 6
ORTEP comparison of estimated H-atom ADPs (122 K) with adjusted neutron results for xylitol. Ellipsoids as in Fig. 2.

the ADPH results are in best overall agreement with these unadjusted neutron results, closely followed by TLS + ONIOM, while SHADE gives slightly worse agreement. TLS + ONIOM and SHADE provide a poor prediction of the ADP for H1: its value alone contributes 50–65% of $\bar{S}$, and we note that this H atom is involved in the shortest hydrogen bond in the crystal (H1$\cdots$O1 = 1.75 Å, compared with H2$\cdots$O2 = 1.82 and H3$\cdots$O2 = 2.04 Å).

1-Methyluracil. Agreement of TLS + ONIOM results with adjusted neutron ADPs is remarkably good, as noted previously (Whitten & Spackman, 2006). The *ORTEP* plot in Fig. 3 for the ADPH method is for model *B* in Table 2 of Roversi & Destro (2004) (model *A* produces almost identical results), and from this it is clear that their approach also yields excellent agreement with the neutron results. The SHADE results are not in such good agreement, and inspection of the figure reveals that this is due to the methyl H atoms, in particular H11, as well as H3 attached to the ring nitrogen N3. In the crystal, the molecules form centrosymmetric dimers *via* N—H$\cdots$O hydrogen bonds (H$\cdots$O = 1.76 Å), and it is clear that the SHADE model is inadequate for these H atoms. For all methods, mean $\Delta U^{\rm iso}$ values (Table 2) are within the range of the $\sigma(U^{ii})$ for the neutron H-atom ADPs (0.0006–0.0013 Å^2).

L-Alanine. Here agreement is best for ADPH and TLS + ONIOM approaches, while the SHADE results are significantly inferior, largely due to the methyl H atoms which contribute 65% of $\bar{S}$ for that method. As observed for α-glycine, the ammonium H atom involved in the shortest hydrogen bond, H3, also shows poor agreement in TLS + ONIOM and SHADE methods (for reference, H3$\cdots$O2 = 1.72, H2$\cdots$O2 = 1.83 and H1$\cdots$O1 = 1.83 Å). For TLS + ONIOM and SHADE, mean $\Delta U^{\rm iso}$ values (Table 2) are well outside the range of 0.0006–0.0019 Å^2 observed for the $\sigma(U^{ii})$ for the neutron H-atom ADPs, and all values are positive, perhaps indicating that these methods systematically overestimate the magnitude of H-atom ADPs for L-alanine. However, as these results are anomalous in comparison with all others in Table 2, it seems more likely that the adjustment with *UIJXN* is less reliable than in the other cases, as it attempts to correct for the very large 37 K difference between the neutron and X-ray experiments.

2-Methyl-4-nitroaniline. For MNA, both TLS + ONIOM and SHADE results are in very good agreement with the adjusted neutron results, and again we note that the worst agreement is found for the hydrogen-bonded proton involved in the shortest hydrogen bond, in this case HN*a* (HN*a*$\cdots$O2 = 2.06 and HN*b*$\cdots$O1 = 2.27 Å). SHADE results for methyl H atoms are again seen to be inferior to the other estimate. For both methods, mean $\Delta U^{\rm iso}$ values are well inside the range of the $\sigma(U^{ii})$ for the neutron H-atom ADPs (0.0009–0.0022 Å^2).

Xylitol. Both TLS + ONIOM and SHADE results are in excellent agreement with neutron ADPs, and in this case agreement for SHADE is the better of the two. In common to both methods, we see that the worst agreement is obtained for two of the methylene protons, H5*a* and H5*b*, as well as for H13, one of the O—H protons. Again, we note that H13 is involved in a short hydrogen-bond contact in the crystal (H13$\cdots$O1 = 1.69, H11$\cdots$O5 = 1.71, H15$\cdots$O3 = 1.72, H12$\cdots$O4 = 1.85 and H14$\cdots$O2 = 1.90 Å).

Several important conclusions emerge from these individual comparisons, and we discuss each of these in turn, with reference to the breakdown by atom type of $\bar{S}$ and average $\Delta U^{\rm iso}$ statistics in Table 3.

(i) Where comparisons can be made with all three estimation approaches, Roversi & Destro's ADPH method yields ADPs in best agreement with adjusted neutron results. For the 17 H atoms in α-glycine, 1-methyluracil and L-alanine, $\bar{S}$ = 0.59 and mean $\Delta U^{\rm iso}$ = −0.0001 Å^2 compared with $\bar{S}$ = 0.60 and mean $\Delta U^{\rm iso}$ = 0.0014 Å^2 for TLS + ONIOM and $\bar{S}$ = 1.22 and mean $\Delta U^{\rm iso}$ = 0.0024 Å^2 for SHADE. The table also provides averages for all atoms, where comparison between TLS + ONIOM and SHADE results suggests that the latter remains inferior.

(ii) Perhaps the main reason for the inferior performance of the SHADE method is due to its description of methyl H atoms, which was noted repeatedly in the individual comparisons above, and for which $\bar{S}$ = 1.51 and mean $\Delta U^{\rm iso}$ = 0.0050 Å^2 for eight atoms, values far worse than observed for either ADPH or TLS + ONIOM results. The large value of mean $\Delta U^{\rm iso}$ = 0.0050 Å^2 hints at the origin of this systematic discrepancy: the SHADE internal mean-square displacements for these atoms are systematically overestimated. Further evidence for the need for reduced internal MSDs for methyl H atoms comes from Weber *et al.* (1991) whose analyses of neutron diffraction data for cholesteryl acetate and 20-methylpregnenediol methanolate yielded average MSDs (taken over 30 methyl H atoms) of 0.0052 Å^2 (C—H stretch), 0.0371 Å^2 (C—C—H out-of-plane) and 0.0188 Å^2 (C—C—H in-plane). The C—H stretch and out-of-plane values are close to those implemented in the SHADE server (0.0038 and 0.0369 Å^2, respectively), but the in-plane value is 23% smaller than the relevant SHADE quantity (0.0245 Å^2) (Madsen *et al.*, 2003).

(iii) Hydrogen-bonded protons also display larger than average values for $\bar{S}$ and $\Delta U^{\rm iso}$ in Table 3. This is especially true for ammonium and amine protons in the TLS + ONIOM method, and for ammonium and aromatic N–H protons in SHADE, but it is also evident in the ADPH results for ammonium H atoms. It has already been noted that the treatment of hydrogen bonding in the TLS + ONIOM method relies entirely on the molecular-mechanics force field, which is used to describe the interactions between the high-level layer (the central molecule of interest) and the low-level layer (the surrounding molecules), and the present analysis emphasizes the inadequacy of the UFF force field (Rappé *et al.*, 1992) used so far for this purpose. The SHADE description of internal MSDs for the aromatic N–H proton in 1-methyluracil is based on the default values of 0.005 Å^2 (bond direction) and 0.020 Å^2 (perpendicular to the bond). Although the default bond-stretch MSD is close to the value of 0.0063 Å^2 derived from the neutron diffraction experiment itself (McMullan & Craven, 1989), default MSDs perpendicular to the bond are considerably greater than the actual neutron diffraction

Table 4
Internal mean-square displacements ($\times 10^4$ Å^2) for SHADE2 derived from neutron diffraction studies.

R.m.s. deviations from mean values are given in parentheses. As noted by Klooster *et al.* (1991) and Weber *et al.* (1991), the distinction between in-plane and out-of-plane is not meaningful for aliphatic C—H H atoms, and these values are assumed to be equal.

Group	Population	Stretch	Out-of-plane	In-plane
—C—H aliphatic	67	48 (26)	148 (33)	
—C—H aromatic	14	47 (32)	232 (55)	146 (36)
—CH—H	142	58 (40)	153 (35)	238 (75)
—CH_2—H	53	57 (39)	367 (73)	182 (33)
—N—H	7	52 (12)	235 (86)	122 (23)
—NH—H	22	51 (19)	200 (104)	138 (29)
—NH_2—H	12	34 (20)	172 (61)	135 (19)
—O—H	23	55 (44)	165 (53)	108 (38)

results of 0.0099 and 0.0122 Å^2. Clearly the SHADE results could be significantly improved by incorporation of specific MSDs for a greater variety of H atoms, such as $N_{aromatic}$—H, $C_{aromatic}$—H, and by revising values for others, such as C_{methyl}—H and $N_{ammonium}$—H.

4. A revised SHADE model

In this section, we attempt to correct the deficiencies noted above for the SHADE method and determine an improved and extended library of internal mean-square displacements. Using this new library, we also explore the possible importance of allowing greater flexibility in the rigid-body description of the heavy-atom skeleton with a segmented rigid-body approach.

4.1. Revised library of internal MSDs: SHADE2

As noted earlier, SHADE uses MSDs from Table 5 of Madsen *et al.* (2003), and for methyl H atoms these represent an average over 14 C—H bonds derived from analyses of neutron diffraction studies on α-D-lyxofuranoside, α-D-xylofuranoside, β-D-arabinofuranoside, methylammonium hydrogensuccinate (MAHS) and methylammonium hydrogenmaleate (MADMA). Inspection of the individual values obtained in those studies reveals that the results for MAHS and MADMA exhibit quite different trends from those for the carbohydrates. Most notably, the five largest values for in-plane MSDs are obtained for the five protons in these structures, and for the three protons in MADMA the in-plane MSDs are considerably greater than the out-of-plane MSDs, in disagreement with all other results used for the SHADE average. These anomalies were in fact noted by Madsen *et al.* in their original work, and from the present analysis and comparison with other methods it is clear that the results for MAHS and MADMA should not be used to estimate typical internal MSDs for methyl H atoms. Simply excluding the five H atoms from these structures results in average internal MSDs of 0.0041 Å^2 (C—H stretch), 0.0364 Å^2 (C—C—H out-of-plane) and 0.0171 Å^2 (C—C—H in-plane), which would reduce the mean ΔU^{iso} value for methyl H atoms by an average of 0.0025 Å^2. In order to further improve and extend the SHADE library, we have also incorporated internal MSDs that were already available in the literature (McMullan & Craven, 1989; Klooster *et al.*, 1991; Kampermann *et al.*, 1995; Luo *et al.*, 1996). As none of these studies reported internal MSDs for hydrogen bound to nitrogen, we analysed ADPs for a further nine nitrogen-containing high-quality structures determined at low temperature using neutron diffraction (Kvick *et al.*, 1977, 1980; Takusagawa *et al.*, 1981; Espinosa *et al.*, 1996; Ellena *et al.*, 1999; Rodrigues *et al.*, 2001; Cole *et al.*, 2002; Cousson *et al.*, 2005; Mata *et al.*, 2006), following the method outlined by Madsen *et al.* (2003). Mean values with associated r.m.s. deviations were computed for chemically similar H atoms and then merged with additional literature results for these atoms (McMullan & Craven, 1989; Klooster *et al.*, 1991; Kampermann *et al.*, 1995; Luo *et al.*, 1996; Madsen *et al.*, 2003).

The results (Table 4) constitute the new SHADE library of internal hydrogen MSDs, and we refer to this library by the acronym SHADE2. A major change from the previous library is a reduction of the methyl hydrogen in-plane vibrations from 0.0245 (115) to 0.0182 (33) Å^2. Apart from the new data for amine and amide H atoms, the large pool of information on hydrogen bound to carbon allowed us to distinguish between aliphatic and aromatic methine groups. Whereas the in-plane vibrations are similar in these groups of methine H atoms, the out-of-plane MSDs of H atoms in aromatic rings are more than 50% larger. However, the r.m.s. deviations accompanying the mean values in Table 4 hint at the inherent limitation of the assumption of transferability of internal mean-square displacements, as well as reflecting the different experimental conditions and treatment of systematic errors in those neutron diffraction experiments.

Table 3 compares the performance of SHADE2 with that of SHADE for the 37 H atoms in the five small-molecule benchmark structures. There is a significant reduction in $\bar{S}$ for almost all atom types and a very small increase in ΔU^{iso} overall; most of the improvement is observed for methyl H atoms and H atoms bound to N and O atoms, while for several other atom types agreement has marginally worsened for these five structures. It is especially notable that agreement of SHADE2 with neutron results is now only slightly inferior to that observed with the TLS + ONIOM approach. Although not shown in the tables, we have also computed mean similarity indices to compare SHADE2 and SHADE against neutron, TLS + ONIOM and ADPH results. We find that $\bar{S}$(SHADE2 : neutron) = 0.66 compared with $\bar{S}$(SHADE : neutron) = 0.89, $\bar{S}$(SHADE2 : TLS + ONIOM) = 0.38 compared with $\bar{S}$(SHADE : TLS + ONIOM) = 0.55, and $\bar{S}$(SHADE2 : ADPH) = 1.05 compared with $\bar{S}$(SHADE : ADPH) = 1.55. The improvement of the SHADE2 library over the original version is considerable, and in particular we note that exceptionally good agreement is obtained between SHADE2 and TLS + ONIOM results and, for the discussion in the following section, we observe that

Table 5
Statistics summarizing agreement between SHADE2 and neutron results for MBADNP, adenosine and Nit(SMe)Ph, and SHADE2 and ADPH results for austdiol, a push–pull ethylene (PPE) and milfasartan.

Figs. 7 and 8 provide molecular structures and atom labels relevant to the definition of libration axes. R_w is the weighted R factor obtained for the rigid or segmented rigid-body fit to ADPs of the heavy atoms, $\bar{S}$ the mean similarity index for the comparison between H-atom ADPs, and ΔU^{iso} ($\times 10^4$ Å^2) the mean deviations of U^{iso} from neutron or ADPH results.

Molecule	Model	Details of rigid groups and libration axes	R_w	$\bar{S}$	ΔU^{iso}
Comparison of SHADE2 with neutron results					
MDADNP	Rigid		0.150	0.35	13
	Segmented-1	2 groups; axis along N1—C7	0.140	0.33	14
	Segmented-2	2 groups; axis through C7, ⊥ to C7—N1 and C7—C1	0.142	0.35	15
Adenosine	Rigid		0.134	0.73	6
	Segmented-1	2 groups; axis along C6—N3	0.087	0.66	8
	Segmented-2	2 groups; axis through C6 and ⊥ to C6—N3 and C6—C7	0.120	0.67	3
Nit(SMe)Ph	Rigid		0.075	1.01	32
	Segmented	2 groups; axis along C1—C2	0.069	0.93	26
Comparison of SHADE2 with ADPH results					
Austdiol	Rigid		0.131	0.52	10
PPE	Rigid		0.204	1.18	24
	Segmented	3 groups; axes along C3—C6; through N2 and ⊥ to N2—C12 and N2—C8; through N1 and ⊥ to N1—C9 and N1—C7	0.139	1.06	27
Milfasartan	Rigid		0.252	1.15	21
	Segmented-1	4 groups; axes along C20—C17; C14—C13; C6—C5; through N2 and ⊥ to N2—C5 and N2—C2	0.171	1.10	28
	Segmented-2	5 groups; axes along C20—C17; C14—C13; C6—C5; C26—C25; through N2 and ⊥ to N2—C5 and N2—C2	0.158	1.16	26

typical agreement between the SHADE2 model and neutron results for these molecules is an $\bar{S}$ value of 1.0 or better.

4.2. SHADE2 and a segmented rigid-body approach

The SHADE server has been further enhanced to allow a segmented rigid-body analysis *via* the approach in the *THMA* program (Schomaker & Trueblood, 1968, 1998). The server can presently handle seven attached rigid groups; details are signalled by a non-standard loop defining the libration axes and rigid groups included in the input CIF file. We have used this approach to explore the possible improvement in H-atom ADPs that may be gained from a segmented rigid-body description of the heavy-atom skeleton, and for this purpose we choose three relatively large molecules with internal degrees of freedom, and for which both X-ray and neutron diffraction results are available: the nucleoside adenosine, the organic NLO material MBADNP, and the organic free radical Nit(SMe)Ph. Table 1 summarizes the relevant experimental details, and molecular structures are depicted in Fig. 7, with labelling of key atoms describing the chosen libration axes. Although a large number of choices can be made for attached rigid groups and internal libration axes, we explore at most two different models to fit ADPs of the heavy atoms; Table 5 summarizes the various models and results, and similarity indices and ADPs for all H atoms are provided in Tables S6–S8 of the supplementary material.

MBADNP. As judged by weighted R factor, R_w, segmented rigid-body fits to heavy-atom ADPs for MDADNP represent only a marginal improvement over the rigid-body fit. Similarity indices indicate extremely good agreement between neutron and SHADE2 ADPs for H atoms, irrespective of the model fitted to the heavy-atom ADPs, and the relatively small mean difference in U^{iso} is in accord with the best results for the five benchmark compounds in Table 3, and just outside the

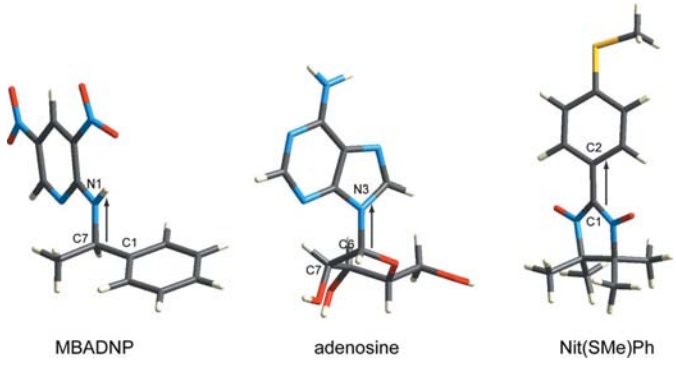

Figure 7
Molecules used for comparison between SHADE2 and neutron results. Atom labels are relevant to description of libration axes for segmented rigid-body analyses (see text).

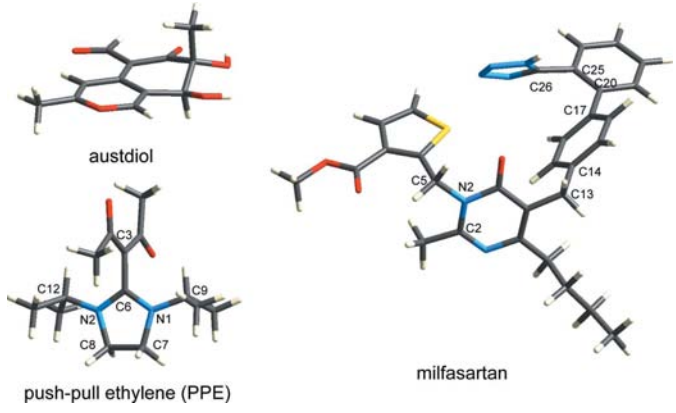

Figure 8
Molecules used for comparison between SHADE2 and ADPH results. Atom labels are relevant to description of libration axes for segmented rigid-body analyses (see text).

range of the $\sigma(U^{ii})$ for the neutron H-atom ADPs (0.0006–0.0011 Å^2).

Adenosine. In contrast to MBADNP, for adenosine, segmented rigid-body descriptions of the heavy-atom skeleton result in a marked improvement in R_w, especially where the libration axis is along the glycosidic bond C6—N3, a model that was also found by Klooster *et al.* (1991) to represent the best fit to their neutron ADPs. However, despite the improved description of the motion of the heavy-atom skeleton, only small changes are observed in the mean similarity index. Inspection of the changes in similarity indices for individual atoms reveals that for some atoms there are large differences between H-atom ADPs derived from the three different models describing the motion of the heavy atoms, and substantial improvements observed for some atoms are accompanied by worsening agreement for others.[2] Mean $\Delta U^{\rm iso}$ values are well within the range of the $\sigma(U^{ii})$ for the neutron H-atom ADPs (0.0011–0.0024 Å^2).

Nit(SMe)Ph. The segmented rigid-body model offers little improvement in R_w for Nit(SMe)Ph and, as observed for adenosine, the mean similarity index shows only marginal improvement. The relatively large mean $\Delta U^{\rm iso}$ values are actually within the range of the $\sigma(U^{ii})$ for the neutron H-atom ADPs for this compound (0.002–0.004 Å^2).

In summary, it would appear that for these three molecular crystals the agreement between SHADE2 and adjusted neutron H-atom ADPs is entirely in accord with the results for the five benchmark systems in Table 3 and the similarity indices suggest that a segmented rigid-body description of the heavy atoms provides a slight advantage in estimating H-atom ADPs for use in a charge-density analysis.

We make one further comparison with the SHADE2 results, this time with H-atom ADPs obtained with ADPH, and for which no neutron diffraction results are presently available as benchmarks. We choose three recent charge-density studies by Destro and co-workers where estimated H-atom ADPs were incorporated in detailed charge-density analyses of low-temperature X-ray diffraction data: the fungal metabolite austdiol (Lo Presti *et al.*, 2006), a twisted push–pull ethylene (PPE) (Forni & Destro, 2003) and the angiotensin II receptor antagonist labelled LR-B/081 (milfasartan) (Destro *et al.*, 2005). For each of these investigations, estimates of ADPs for H atoms were obtained using the basic procedure reported by Roversi & Destro (2004) but, as the precise details have not been reported previously, they are included here as they are directly relevant to the comparison with the SHADE2 results; Table 5 summarizes the relevant statistics and similarity indices for all atoms are given in the supplementary material, Tables S9–S11.

Austdiol. The rigid-body analysis performed by Lo Presti *et al.* (2006) excluded the seven exocyclic C and O atoms, and experimental group vibrational frequencies (Grasselli & Ritchey, 1975) were used to provide estimates of internal contributions to the H-atom ADPs. For this molecule, only a rigid-body fit is possible (see Fig. 8) and in SHADE2 all heavy atoms were used in this analysis. From Tables 5 and S9, we see that the agreement between H-atom ADPs obtained from these two procedures is excellent.

Push–pull ethylene (PPE). A rigid-body analysis was used by Forni & Destro (2003) to obtain external contributions to the H-atom ADPs. For this purpose, the molecule (Fig. 8) was split into four moieties (the pentanedione group; the imidazolidinylidene ring plus atom C3; and the two isopropyl groups, including four atoms of the imidazolidinylidene ring in each case) and each was treated as an independent rigid body. This is not the same as the segmented rigid-body analysis embodied in THMA and used by the SHADE server. Internal contributions were derived using scaled vibrational frequencies from an HF/6-31G** optimized geometry of the free PPE molecule. For the SHADE2 results in the present work, a single segmented rigid-body model was explored for comparison with a rigid-body description, and it results in a substantial lowering of R_w from 0.204 to 0.139 (Table 5), a result similar to that observed for adenosine. Mean similarity indices summarizing the agreement of SHADE2 H-atom ADPs with ADPH results are satisfactory: 1.18 for a rigid-body model, improving slightly to 1.06 with a segmented rigid-body description of the heavy-atom skeleton. However, the mean difference in $U^{\rm iso}$ between the two sets of results is ~0.0025 Å^2, indicating that the SHADE2 ADPs are considerably and systematically higher than those obtained by ADPH.

Milfasartan. This is by far the largest molecule considered in our study, and Table 5 summarizes the SHADE2 results using a rigid-body model and two different segmented rigid-body descriptions of the heavy-atom skeleton. Both segmented rigid-body descriptions show considerably better fits to the heavy-atom ADPs than does the rigid-body model, and the more complex model with five attached rigid groups appears to be the better of the two. For milfasartan, the ADPH procedure implemented by Destro *et al.* (2005) was based on a rigid-body fit to the ADPs of heavy atoms of separate fragments, in the same manner as PPE, and five groups were used for this purpose: the thiophene group including the COOMe heavy atoms; the pyrimidinone ring plus butylic chain; the two phenyl groups, each with one additional outer C atom bonded to it; and the tetrazole ring plus atom C25 (see Fig. 8). Internal contributions to H-atom ADPs were based on experimental spectroscopic information. From Table 5, we see that the agreement between ADPH and SHADE2 results is very similar to that obtained for PPE, with $\bar{S}$ close to 1.1 and the mean difference in $U^{\rm iso}$ around 0.0025 Å^2 (*i.e.* the SHADE2 estimated ADPs are again systematically greater than those obtained from ADPH). As noted for adenosine, Nit(SMe)Ph and PPE, a segmented rigid-body modelling of the heavy-atom ADPs can result in improved agreement, but this is not necessarily the case.

[2] A similar outcome was found in TLS + ONIOM calculations on adenosine using potential-derived atomic charges and a 6-31G** basis set for the inner layer (Osborne, 2006). In that work, $\bar{S}$(TLS + ONIOM : neutron) = 0.79 for a rigid-body model, and 0.70 for a segmented rigid-body model. This represents agreement similar to that obtained with SHADE2, in line with other results in Table 2.

5. Concluding remarks

We initiated this study with the aim of comparing, for five relatively small molecules, ADPs for H atoms estimated using recently described procedures, both among themselves and with neutron diffraction results. The results convincingly demonstrate that all methods – ADPH, TLS + ONIOM and SHADE – are capable of giving excellent results for these benchmark systems, but it appears that ADPH yields marginally better agreement with neutron results, followed by TLS + ONIOM, with the SHADE approach giving markedly inferior results, especially for methyl groups. Having identified systematic discrepancies for these and other atom types, we have analysed neutron diffraction ADPs for a substantial number of additional molecular crystals to obtain a revised and extended library of internal H-atom MSDs for use with Madsen's SHADE web server, and we identify these results as SHADE2.

The improvement of SHADE2 over the original SHADE results is substantial, and it is clear that this is the most readily – and widely – applicable of the three approximate procedures. In a comparison with neutron ADPs for three additional molecular crystals, SHADE2 has been shown to provide estimates of H-atom ADPs in excellent agreement with adjusted neutron results, with a mean similarity index for all eight systems of 0.68. Further comparison with ADPs obtained using Roversi & Destro's ADPH procedure for a further three molecules also revealed excellent agreement.

Using the SHADE2 approach, which clearly works well for rigid molecules, we have explored the possible improvements in H-atom ADPs that might arise from a segmented rigid-body description of the heavy atoms to deduce external contributions to H-atom MSDs. The outcome seems clear-cut: despite a segmented rigid-body model often yielding a much better fit to the heavy-atom ADPs, and presumably being a better model of the molecular motion, there is only modest improvement in the agreement between estimated and neutron ADPs. This result can be understood on the basis that, for H atoms, $U^{ij}_{\rm internal}$ is typically much greater than $U^{ij}_{\rm external}$ and, the lower the temperature, the greater the difference between these contributions. It can also be seen from the weak correlation of mean $\Delta U^{\rm iso}$ values (Table 5) with the number of methyl groups in the molecules that SHADE2 still tends to overestimate $U^{\rm iso}$ for methyl H atoms, and this suggests that there is room for further improvement of the set of internal mean-square displacements (Table 4).

The TLS + ONIOM method is the most time-consuming of the three procedures considered in this comparison but it is clearly capable of providing excellent agreement with adjusted neutron diffraction results. It has some obvious deficiencies, but can be streamlined in many instances by using potential-derived charges for isolated molecules rather than more expensive field-derived charges obtained from periodic Hartree–Fock calculations, and different force fields (or perhaps just the description of the hydrogen-bond potential) deserve detailed investigation.

We recommend the SHADE2 library, now incorporated in the SHADE web server, as a routine procedure for deriving estimates of H-atom ADPs suitable for use in charge-density studies on molecular crystals. Widespread use of these ADPs in analyses aimed at deriving quantitative information from experimental electron densities should reveal remaining deficiencies, and perhaps finally overcome the inherent bias in the majority of such studies.

Finally, although our comparisons with neutron diffraction results made use of Blessing's adjustment procedure, that approach provides little insight into the origin of discrepancies between X-ray and neutron ADPs. Apart from the use of different samples, and differences in absorption, extinction, thermal diffuse scattering and temperature, the actual conditions of the measurements (*e.g.* adopted scan width in step-scanning experiments and incident-beam homogeneity) play a crucial role and make difficult any comparison between the two sets of results. These considerations have been discussed by Blessing (1995) and in more detail by Wilson (2000). Excellent agreement between X-ray and neutron ADPs can be obtained, especially by exploiting the advantages afforded by measurements near 10 K (Larsen, 1991; Iversen *et al.*, 1996) but, if a significant comparison between X-ray and neutron ADPs is sought, experimental protocols will need to be devised and followed to minimize, if not cancel, the sources of systematic errors. A comparison of this kind would seem to be an ideal project for one of the IUCr Commissions.

This work has been supported by the Australian Research Council. The authors are grateful to Wim Klooster (Nanyang Technological University, Singapore), Sébastien Pillet (Université Henri Poincaré, Nancy) and Christian Hübschle (Free University of Berlin) for providing unpublished results, and Bob Blessing and Nicholas Furlani (Hauptman–Woodward Institute, Buffalo) for the use of their digitized structural data for amino acids.

References

Bader, R. F. W. (1990). *Atoms in Molecules – A Quantum Theory*. Oxford University Press.
Baert, F., Schweiss, P., Heger, G. & More, M. (1988). *J. Mol. Struct.* **178**, 29–48.
Blessing, R. H. (1995). *Acta Cryst.* B**51**, 816–823.
Buschmann, J., Koritsanszky, T., Lentz, D., Luger, P., Nickelt, N. & Willemsen, S. (2000). *Z. Kristallogr.* **215**, 487–494.
Chen, L. & Craven, B. M. (1995). *Acta Cryst.* B**51**, 1081–1097.
Cole, J. M., Goeta, A. E., Howard, J. A. K. & McIntyre, G. J. (2002). *Acta Cryst.* B**58**, 690–700.
Cousson, A., Nicolaï, B. & Fillaux, F. (2005). *Acta Cryst.* E**61**, o222–o224.
Dapprich, S., Komáromi, I., Byun, K. S., Morokuma, K. & Frisch, M. J. (1999). *J. Mol. Struct.* **461–462**, 1–21.
Destro, R., Marsh, R. E. & Bianchi, R. (1988). *J. Phys. Chem.* **92**, 966–973.
Destro, R. & Merati, F. (1995). *Acta Cryst.* B**51**, 559–570.
Destro, R., Roversi, P., Barzaghi, M. & Marsh, R. E. (2000). *J. Phys. Chem. A*, **104**, 1047–1054.
Destro, R., Soave, R., Barzaghi, M. & Lo Presti, L. (2005). *Chem. Eur. J.* **11**, 4621–4634.

Dittrich, B. & Spackman, M. A. (2007). *Acta Cryst.* A**63**, 426–436.
Eisenstein, M. (1979). *Acta Cryst.* B**35**, 2614–2625.
Eisenstein, M. (1988). *Acta Cryst.* B**44**, 412–426.
Eisenstein, M. & Hirshfeld, F. L. (1983). *Acta Cryst.* B**39**, 61–75.
Ellena, J., Goeta, A. E., Howard, J. A. K., Wilson, C. C., Autino, J. C. & Punte, G. (1999). *Acta Cryst.* B**55**, 209–215.
Espinosa, E., Lecomte, C., Molins, E., Veintemillas, S., Cousson, A. & Paulus, W. (1996). *Acta Cryst.* B**52**, 519–534.
Fkyerat, A., Guelzim, A., Baert, E., Paulus, W., Heger, G., Zyss, J. & Périgaud, A. (1995). *Acta Cryst.* B**51**, 197–209.
Flaig, R., Koritsanszky, T., Zobel, D. & Luger, P. (1998). *J. Am. Chem. Soc.* **120**, 2227–2238.
Forni, A. & Destro, R. (2003). *Chem. Eur. J.* **9**, 5528–5537.
Grasselli, J. G. & Ritchey, W. M. (1975). Editor. *Atlas of Spectral Data and Physical Constants for Organic Compounds*, 2nd ed. Cleveland: CRC Press.
Hamzaoui, F., Baert, F. & Wojcik, G. (1996). *Acta Cryst.* B**52**, 159–164.
Hirshfeld, F. L. (1976). *Acta Cryst.* A**32**, 239–244.
Hirshfeld, F. L. & Hope, H. (1980). *Acta Cryst.* B**36**, 406–415.
Hübschle, C. B. (2007). PhD thesis, Freie Universität Berlin, Germany.
Iversen, B. B., Larsen, F. K., Figgis, B. N., Reynolds, P. A. & Schultz, A. J. (1996). *Acta Cryst.* B**52**, 923–931.
Kampermann, S. P., Sabine, T. M., Craven, B. M. & McMullan, R. K. (1995). *Acta Cryst.* A**51**, 489–497.
Klooster, W. T. & Craven, B. M. (1992). *Biopolymers*, **32**, 1141–1154.
Klooster, W. T., Craven, B. M., Chakoumakos, B. C. & Johnson, C. K. (1996). *Am. Crystallogr. Assoc. Annu. Meet.*, p. 274.
Klooster, W. T., Ruble, J. R., Craven, B. M. & McMullan, R. K. (1991). *Acta Cryst.* B**47**, 376–383.
Koritsanszky, T., Buschmann, J., Lentz, D., Luger, P., Perpetuo, G. & Röttger, M. (1999). *Chem. Eur. J.* **5**, 3413–3420.
Koritsanszky, T., Zobel, D. & Luger, P. (2000). *J. Phys. Chem. A*, **104**, 1549–1556.
Koritsanszky, T. S. & Coppens, P. (2001). *Chem. Rev.* **101**, 1583–1627.
Kvick, Å. (1993). Personal communication to R. Destro.
Kvick, Å., Al-Karaghouli, A. R. & Koetzle, T. F. (1977). *Acta Cryst.* B**33**, 3796–3801.
Kvick, Å., Canning, W. M., Koetzle, T. F. & Williams, G. J. B. (1980). *Acta Cryst.* B**36**, 115–120.
Larsen, F. K. (1991). *The Application of Charge Density Research to Chemistry and Drug Design*, edited by G. A. Jeffrey & J. F. Piniella, pp. 187–208. New York: Plenum Press.
Lo Presti, L., Soave, R. & Destro, R. (2006). *J. Phys. Chem. B*, **110**, 6405–6414.
Luo, J., Ruble, J. R., Craven, B. M. & McMullan, R. K. (1996). *Acta Cryst.* B**52**, 357–368.
Madsen, A. Ø. (2006). *J. Appl. Cryst.* **39**, 757–758.
Madsen, A. Ø., Mason, S. & Larsen, S. (2003). *Acta Cryst.* B**59**, 653–663.
Madsen, A. Ø, Sørensen, H. O., Flensburg, C., Stewart, R. F. & Larsen, S. (2004). *Acta Cryst.* A**60**, 550–561.
Mata, I., Espinosa, E., Molins, E., Veintemillas, S., Maniukiewicz, W., Lecomte, C., Cousson, A. & Paulus, W. (2006). *Acta Cryst.* A**62**, 365–378.
May, E., Destro, R. & Gatti, C. (2001). *J. Am. Chem. Soc.* **123**, 12248–12254.
McMullan, R. K., Benci, P. & Craven, B. M. (1980). *Acta Cryst.* B**36**, 1424–1430.
McMullan, R. K. & Craven, B. M. (1989). *Acta Cryst.* B**45**, 270–276.
Osborne, S. T. (2006). Honours thesis, University of Western Australia, Australia.
Pillet, S., Souhassou, M., Pontillon, Y., Caneschi, Y., Gatteschi, D. & Lecomte, C. (2001). *New J. Chem.* **25**, 131–143.
Puig-Molina, A., Alvarez-Larena, A., Piniella, J. F., Howard, S. T. & Baert, F. (1998). *Struct. Chem.* **9**, 395–402.
Rappé, A. K., Casewit, C. J., Colewell, K. S., Goddard, W. A. & Skiff, W. M. (1992). *J. Am. Chem. Soc.* **114**, 10024–10035.
Rodrigues, B. L., Tellgren, R. & Fernandes, N. G. (2001). *Acta Cryst.* B**57**, 353–358.
Roversi, P., Barzaghi, M., Merati, F. & Destro, R. (1996). *Can. J. Chem.* **74**, 1145–1161.
Roversi, P. & Destro, R. (2004). *Chem. Phys. Lett.* **386**, 472–478.
Schomaker, V. & Trueblood, K. N. (1968). *Acta Cryst.* B**24**, 63–76.
Schomaker, V. & Trueblood, K. N. (1998). *Acta Cryst.* B**54**, 507–514.
Soave, R., Barzaghi, M. & Destro, R. (2007). *Chem. Eur. J.* **13**, 6942–6956.
Svensson, M., Humbel, S., Froese, R. D. J., Matsubara, T., Sieber, S. & Morokuma, K. (1996). *J. Phys. Chem.* **100**, 19357–19363.
Takusagawa, F., Koetzle, T. F., Kou, W. W. H. & Parthasarathy, R. (1981). *Acta Cryst.* B**37**, 1591–1596.
Vreven, T., Byun, K. S., Komáromi, I., Dapprich, S., Montgomery, J. A., Morokuma, K. & Frisch, M. J. (2006). *J. Chem. Theory Comput.* **2**, 815–826.
Vreven, T., Morokuma, K., Farkas, O., Schlegel, H. B. & Frisch, M. J. (2003). *J. Comput. Chem.* **24**, 760–769.
Weber, H.-P., Craven, B. M., Sawzik, P. & McMullan, R. K. (1991). *Acta Cryst.* B**47**, 116–127.
Whitten, A. E., McKinnon, J. J. & Spackman, M. A. (2006). *J. Comput. Chem.* **27**, 1063–1070.
Whitten, A. E. & Spackman, M. A. (2006). *Acta Cryst.* B**62**, 875–888.
Williams, R. V., Gadgil, V. R., Luger, P., Koritsanszky, T. & Weber, M. (1999). *J. Org. Chem.* **64**, 1180–1190.
Wilson, C. C. (2000). *Single Crystal Neutron Diffraction from Molecular Materials.* Singapore: World Scientific.
Wilson, C. C., Myles, D., Ghosh, M., Johnson, L. N. & Wang, W. (2005). *New J. Chem.* **29**, 1318–1322.